Improving the heat transfer efficiency of synthetic oil with silica nanoparticles

Elena V. Timofeeva[1*]
Michael R. Moravek[2]
Dileep Singh[2]

[1]Energy Systems Division
[2]Nuclear Engineering Division
Argonne National Laboratory, Argonne, IL 60439, USA
(E-mail: etimofeeva@anl.gov)

Argonne National Laboratory

Argonne, IL 60439, USA

(E-mail: etimofeeva@anl.gov)

April 2011

The submitted manuscript has been created by Argonne National Laboratory, a U.S. Department of Energy laboratory managed by UChicago Argonne, LLC, under Contract No. DE-AC02-06CH11357 with the U.S. Department of Energy. The U.S. Government retains for itself, and others acting on its behalf, a paid-up, nonexclusive, irrevocable worldwide license in said article to reproduce, prepare derivative works, distribute copies to the public, and perform publicly and display publicly, by or on behalf of the Government

To be submitted to JOURNAL OF COLLOID AND INTERFACE SCIENCE

Improving the heat transfer efficiency of synthetic oil with silica nanoparticles

Elena V. Timofeeva[1*], Michael R. Moravek[2], Dileep Singh[2]
[1]Energy Systems Division
[2]Nuclear Engineering Division
Argonne National Laboratory, Argonne, IL 60439, USA
(E-mail: etimofeeva@anl.gov)

Abstract

The heat transfer properties of synthetic oil (Therminol 66) used for high temperature applications was improved by introducing the 10 nm silicon dioxide nanoparticles. Stable suspensions of inorganic nanoparticles in non-polar fluid were prepared using cationic surfactant (benzalkonium chloride). The effects of nanoparticle and surfactant concentrations on thermo-physical properties (viscosity, thermal conductivity and total heat absorption) of nanofluids were investigated. The surfactant-to-nanoparticle (SN) ratio was optimized for higher thermal conductivity and lower viscosity which are both critical for efficient heat transfer. The rheological behavior of nanofluids was correlated to agglomerate sizes, which were shown to vary with SN ratio and temperatures. Conditions of ultrasonic treatment were studied and the temporary decrease of agglomerate sizes from equilibrium size (characteristic to SN ratio) was demonstrated. The heat transfer efficiency of the formulated nanofluids was estimated from the experimental data and fluid dynamic equations for both turbulent and laminar flow regimes.

Keywords: heat transfer fluid, synthetic oil, therminol, nanofluid, silica, silicon oxide, nanoparticles, surfactant, thermal conductivity, viscosity, total heat, heat transfer efficiency

Introduction

The operating temperatures in many process applications range from 150°C to 400°C, and the requirements to heat transfer fluids include stability, sufficient energy transfer and service ratings for the mechanical components. The use of proper heat transfer fluid can be safer and more efficient than steam, electrical, or direct fire heating methods, and also can provide more uniform heat delivery and removal. Amongst the high temperature heat transfer fluids the molecular structures of synthetic (aromatic) oils provide higher stability at elevated temperatures than hot (paraffinic hydrocarbons) or silicone oils. The synthetic oils also offer the highest thermal conductivity amongst the high temperature heat transfer fluids (~0.1 W/mK), but it is still very low compared to thermal conductivity of water (~0.6 W/mK at room temperature) and also decreases with increasing temperatures.

The introduction of nano-sized particles to heat transfer fluids (nanofluids) is an emerging thermal management concept with implications in many disciplines including power generation, transportation, microelectronics, chemical engineering, aerospace and manufacturing [1-10]. Nanoparticles have thermal conductivities that are significantly higher than base fluids, they remain in suspension, and contribute to the thermo-physical properties of the system while mitigating problems associated with erosion, sedimentation and clogging, as observed for suspension of micron size particles. A large variety of nanoparticle suspensions with different nanoparticle materials, shapes, sizes and concentrations have been extensively studied in last decade; however majority of studies have been conducted in polar base fluids, mostly water, ethylene glycol (EG) and their mixtures. There are limited studies on nanofluids in organic and mineral oils for applications such as heat transfer [11-21], friction reduction [22-23], and enhancement of the breakdown voltage [24-25].

The heat transfer coefficients (*h*) are used for evaluation and efficiency comparison of the heat transfer fluids. A fluid with a substantial heat transfer coefficient advantage may allow reduction in sizing of the system equipment, increase the production output, and/or reduce the energy costs. At a specific temperature, flow velocity, and a pipe diameter, a fluid's heat transfer coefficient can be calculated using its density, viscosity, thermal conductivity and specific heat [26].

Although some work has been done with nanoparticle suspensions in organic fluids, the literature lacks studies on the effects of nanoparticle additions to the high temperature heat transfer fluids, especially aromatic synthetic oils. In this study we assess the possible benefits of adding silicon dioxide nanoparticles and surfactant to the aromatic high temperature heat transfer fluid. The effects of the nanoparticles and surfactant concentration on viscosity, thermal conductivity and total heat adsorption of suspensions were studied in two different nanofluid series. The experimental data were used to estimate the heat transfer efficiency in a wide temperature range and to guide the optimization of the nanofluid composition for a better heat transfer performance.

Materials and Methods

The silicon dioxide (silica) nanopowder with average particle sizes of 10 nm (NanoAmorphous Materials, Inc.) was dispersed in the synthetic heat transfer fluid Therminol 66 (TH66) (Solutia, Inc.) with benzalkonium chloride (Acros Organics) as a surfactant. The weight (wt) and volume (vol) percentages used throughout the manuscript refer to the weight and the volume of the resulting nanofluid. Surfactant was dispersed into the base fluid first, followed by introduction of the nanopowder. Mixture was homogenized by continuous stirring with a

magnetic bar and sonicated 10 times (~80W output power, 50% duty cycle, Branson Sonifier S-450) for five minutes each time. Continuous ultrasonic treatment increased the temperature of suspensions, which was monitored to stay below 65°C (initial sonication conditions). The nanofluid was equilibrated to room temperature between the treatments. To investigate the effect of sonication conditions on the nanofluid properties the duration and the number of sonications were increased for some nanofluids.

The effective thermal conductivity of nanoparticle suspensions was measured using the transient hot wire based thermal property analyzer (Model KD2pro, Decagon Devices, Inc.). The reported values represent the average of at least 20 measurements.

The viscosity of the nanofluids was measured at temperatures ranging from 15 to 135°C using a Brookfield DV-II+ rotational type viscometer with the SC4-18 spindle (Brookfield Engineering Laboratories, Inc.).

The total heat adsorption by nanofluids and pure materials were measured using the differential scanning calorimeter Q20 (TA Instruments, Inc.). Measurements were performed in hermetic aluminum pans using ~5 mg of nanofluid sample with temperature scans between 35-250°C with 10°C per minute heating/cooling rate.

The sizes of nanoparticle agglomerates were approximated using the dynamic light scattering (DLS) at a 90° scattering angle with a 90Plus/BIMAS particle size analyzer (Brookhaven Instruments Corp., NY). All samples were diluted ~ 1000 times to avoid multiple scattering effects.

Results and Discussion

1. The effect of nanoparticle concentration

The particle concentration series was prepared with 5 wt% of surfactant and SiO_2 concentrations of ~1.2, 3.6, 5.0 and 7.0 vol%. Nanofluids appeared stable without any visual phase separation for at least a week. The viscosity of nanofluids measured at various temperatures increased non-linearly with particle concentration (Fig. 1). Suspension with 1.2 vol% demonstrated Newtonian, shear independent behavior in the whole tested temperature range, similar to the TH66 base fluid behavior. Nanofluid with 3.6 vol% of SiO_2 showed shear thinning non-Newtonian behavior at temperatures below 65°C (multiple markers on Fig. 1 refer to various shear stresses) while at higher temperatures the Newtonian behavior is observed. Similar effects of nanoparticle concentration were observed at room temperature in viscosity of aluminum oxide nanofluids in PAO oil [12-13], showing Newtonian behavior at 1 vol% and the shear dependent behavior at nanoparticle concentrations of 3 vol%. The change from non-Newtonian to Newtonian behavior with increasing temperatures was also described for SiO_2 suspensions in EG/H_2O mixtures [27]. Non-linear increase in viscosity with concentration indicated agglomeration of particles. Extended nanoparticle agglomerates restrict the fluid flow resulting in a dramatic viscosity increase and non-Newtonian shear dependent behavior. The balance of acting forces (Brownian motion, viscous resistance, intermolecular Van-der-Waals interaction, and electrostatic interactions between ions and dipoles of the nanoparticles and the fluid [28]) defines if particles move independently (well dispersed suspensions) or ensembles of particles move together (agglomerated suspensions) [29]. Increase in kinetic energy of individual nanoparticles at elevated temperatures can weaken some types of particle-particle interactions, resulting in de-agglomeration of clusters, non-Newtonian to Newtonian change in behavior and lower viscosity increases.

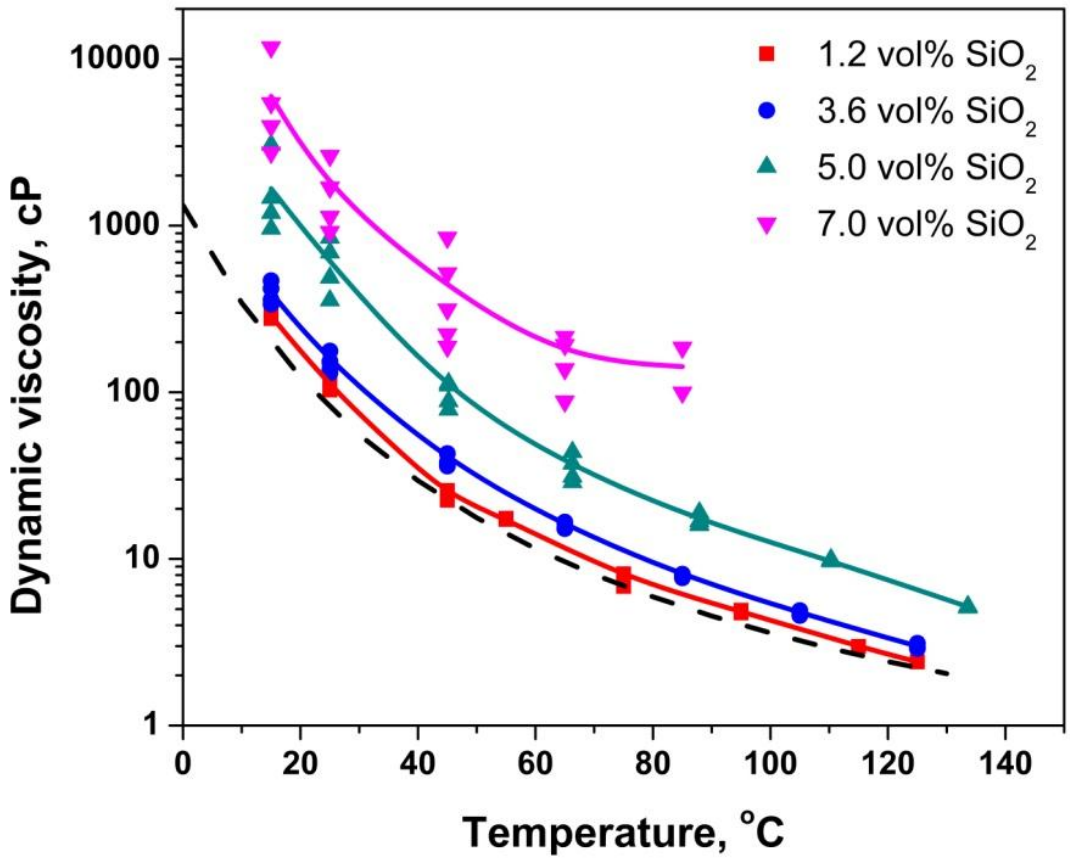

Figure 1. Temperature dependence of the dynamic viscosity of TH66 based nanofluids at various SiO_2 concentrations and 5 wt% of surfactant. Multiple symbols of the same type and color represent the viscosity at shear stress from ~10 to ~40 D/cm^2 with higher viscosity at lower shear stress.

The percentage viscosity increase in SiO_2/TH66 nanofluids was found to be a temperature dependent showing that the viscosity of suspensions becomes closer to the viscosity of the base fluid with the increase in the temperature similar to the trends reported in the literature [30-31]. In case of 1.2 vol% at 15°C, nanofluid viscosity was 23% higher than pure TH66, and at 125°C the nanofluid was only 8% more viscous than the base fluid at the same temperature. Viscosity of the 3.6 vol% suspension ranged from 70% more viscous at 15°C down to only 30% more

viscous at 125°C. This phenomenon is most likely related to de-agglomeration of flow restricting clusters at elevated temperatures.

The suspensions with 5.0 and 7.0 vol % of SiO_2 were significantly more viscous than the base fluid. Very strong shear rate dependence indicated extended nanoparticle agglomerates that make suspension more sensitive to shear due to the flow-induced alignment [32]. Since the surfactant amount maintained constant in the concentration series the surfactant-to-nanoparticle (SN) ratio was lower at high particle concentrations, which resulted in stronger agglomeration.

A continuous increase in viscosity of 7.0 vol% nanofluid was observed at temperatures above 65°C. This is believed to be a strong evidence of insufficiently low SN ratio: due to non-miscible nature of non-polar fluid and inorganic nanoparticles Brownian collisions at elevated temperatures result in continuous particle agglomeration and increase in viscosity [33]. At sufficient SN ratio the particle collisions are mediated through the adsorbed layer of surfactant and the temperature driven agglomeration can be avoided, like it was observed at lower particle concentrations.

The thermal conductivity of suspensions linearly increased in proportion to the volume concentration of nanoparticles (ϕ) (Fig. 2), as predicted by the effective medium theory (EMT) for spherical particles [34]: $\frac{k_{\mathrm{nf}}}{k_0} = 1 + \frac{3(k_p - k_0)}{k_p + 2k_0}\phi$, where k_{nf}, k_p and k_0 are the thermal conductivities of the nanofluid, the particle material and the base fluid correspondingly. The thermal conductivity of amorphous silicon oxide (1.2 W/mK) is ~10 times higher than the thermal conductivity of TH66 at room temperature (0.117 W/mK). Although we saw a strong agglomeration in the concentrated SiO_2/TH66 nanofluids, no abnormal increase in thermal conductivity due to agglomeration was observed in this series despite the reports that

agglomerates can provide percolation pathways for heat conduction that improve the thermal conductivity above the EMT predictions [35].

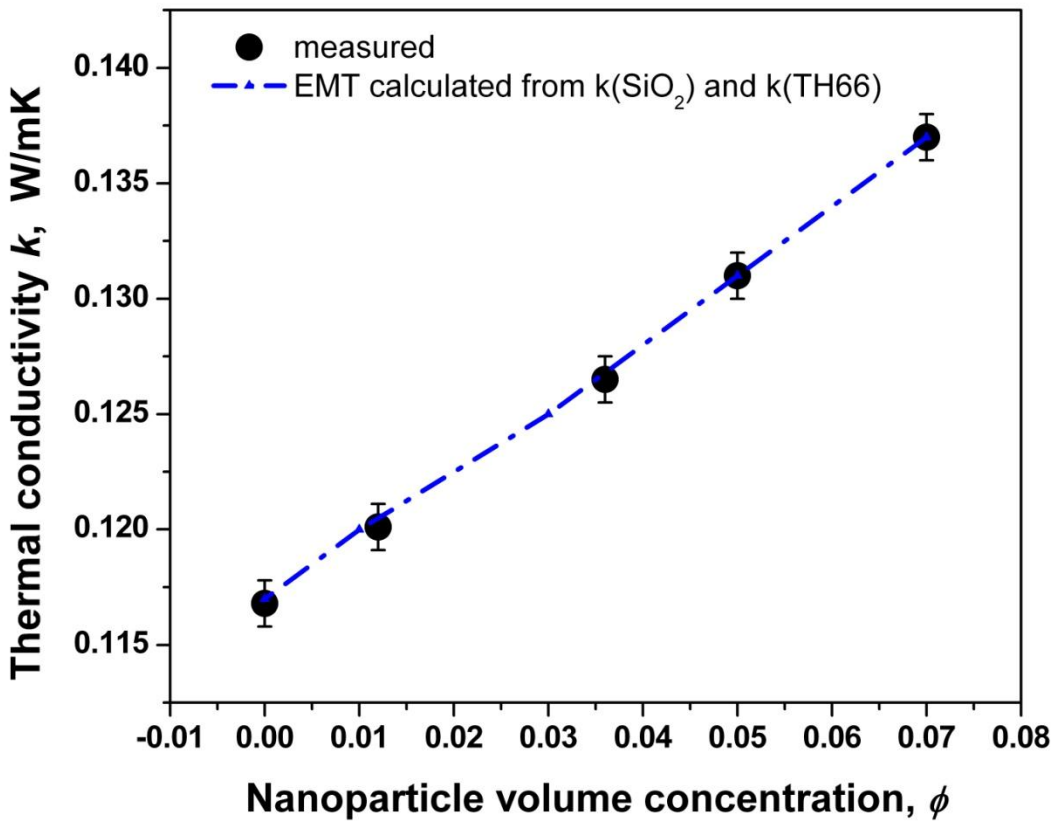

Figure 2. The thermal conductivity of SiO_2 suspensions in TH66 with various particle concentrations and 5 wt% of the surfactant. Dash and dash-dot lines represents the thermal conductivity values calculated from EMT.

The thermal stability and heat absorption by SiO_2/TH66 suspensions were studied by DSC thermal cycling between 35 and 250°C (Fig. 3). The DSC curves were reproducible from cycle to cycle and from sample to sample. No endothermic or exothermic peaks were observed in the studied temperature range, which confirms the stability of suspensions. A good agreement was observed between the total heat absorption/retention during heating and cooling cycles (insert to

Fig. 3). The total heat flow decreased as the concentration of SiO_2 nanoparticles increased, as was expected due to the lower specific heat of nanoparticle material.

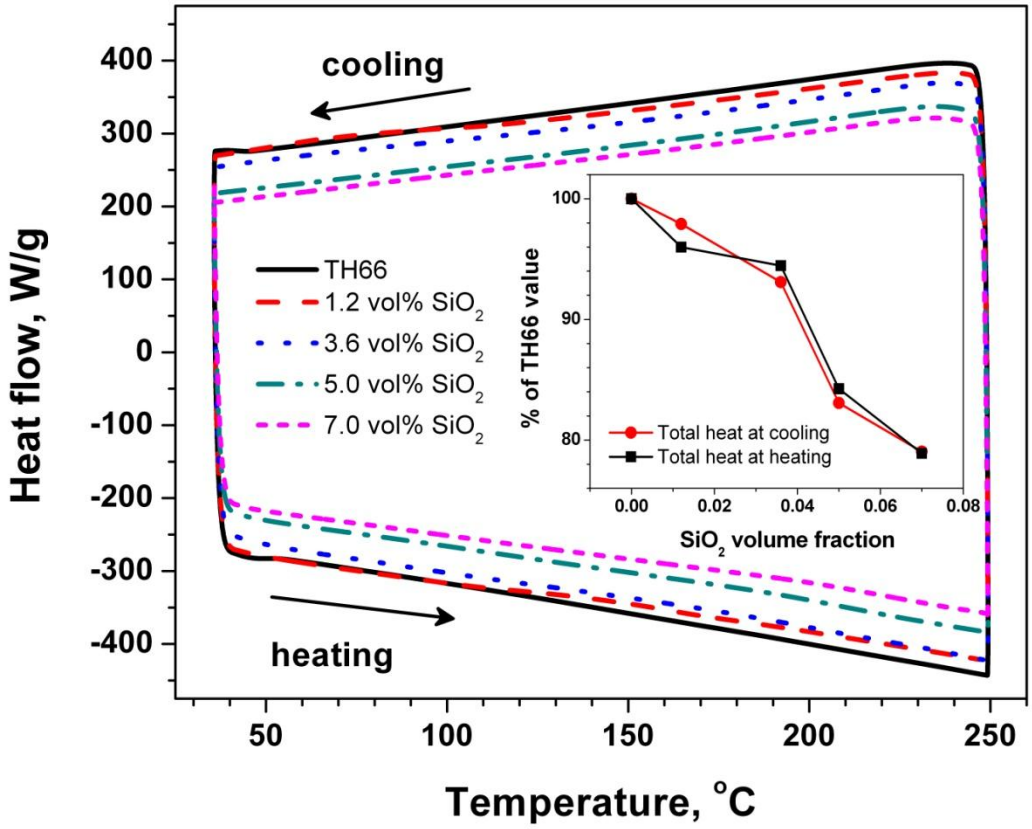

Figure 3. DSC curves of heating and cooling cycles of SiO_2/TH66 suspensions at various particle concentrations (temperature ramp 10°C/min). The insert illustrates total heat adsorption between 35 and 250°C compared to pure TH66 as a function of nanoparticle concentration.

2. Surfactant Concentration

The surfactants are used to control the strength of particle-particle interactions and dispersion/agglomeration of particles in suspension [32, 36-37]. Dispersing inorganic nanoparticles (silicon oxide) in a non-polar organic fluid (TH66) requires a surfactant that would adhere to oxide surface and be miscible with the non-polar fluid. Accounting for the negative

surface charges of silica [38] several cationic surfactants (benzethonium chloride, cetyl trimethylammonium bromide, and benzalkonium chloride) were tested in the preliminary series, and benzalkonium chloride showed the best dispersion stability for SiO_2 in TH66. Therefore benzalkonium chloride was chosen for detailed studies of SiO_2/TH66 nanofluids. Significant effort in this work was put to optimize the surfactant-to-nanoparticle ratio to achieve a desirable for a heat transfer fluid low viscosity.

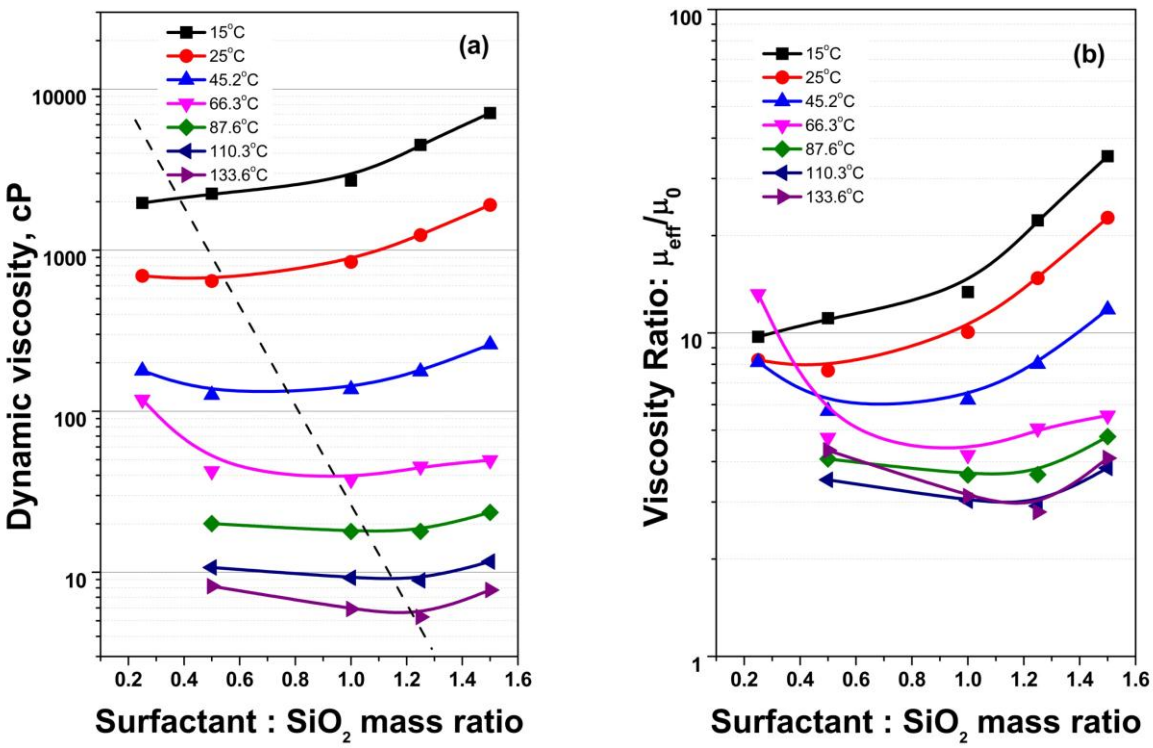

Figure 4. Viscosity (a) and viscosity ratio (b) of 5 vol% SiO_2/TH66 suspensions at various surfactant-to-nanoparticle ratio. Viscosity values at 20 D/cm^2 shear stress are used to compare the results at various temperatures and suspensions compositions.

The effect of SN ratio on viscosity and thermal conductivity was investigated for suspensions with 5.0 vol% of SiO_2 nanoparticles. The range of SN ratio was approximated from the total surface area per gram of nanoparticles using the adsorption model with ”laying flat” (SN 0.37:1) and compacted “standing up” (SN 1.16:1) layers of the surfactant molecules. It is important to

note here that the SN mass ratios used in the paper are specific for the SiO_2 particle size (10 nm) and need to be adjusted for a different particle diameters and material density.

The comparison of non-Newtonian viscosities of 5 vol% of SiO_2 nanofluids at various SN ratios was conducted at fixed shear stress of 20 D/cm^2. As the SN ratio increased the viscosity of nanofluids underwent minimum and increased at the excess amount of the surfactant (Fig. 4a). The SN ratio that corresponds to minimum viscosity varied with the temperature from less than 0.25:1 at 15°C to 1.25:1 at 130°C. Although the SN ratio 0.25:1 showed lowest viscosity of suspension at 15°C, the temperature increase above 65°C resulted in a continuous viscosity increase with time negating any further data collection for that fluid (Fig. 4a and 4b). As it was suggested previously the fluid thickening is most likely a result of temperature driven agglomeration of nanoparticles at insufficient SN ratios. In suspensions with higher SN ratio no temperature driven agglomeration was observed even at highest tested temperatures. Therefore, it is suggested that a minimum surface coverage with a surfactant is required to prevent the nanoparticle agglomeration as they collide in Brownian motion. The viscosity ratio of nanofluids vs. base fluid decreased with temperature almost at all SN ratios (Fig. 4b), similar to the trend observed in the concentration series.

The SN ratio also affected the thermal conductivity of nanofluids (Fig. 5). The thermal conductivity of TH66 and the surfactant are comparable due to similarities in chemical structure, and the surfactant should not represent an obstacle for heat flow. The base fluid with the maximum amount of surfactant used in the series (1.5:1 SN mass ratio for 5 vol% of SiO_2, i.e. 20 wt% of surfactant) was tested along with nanofluids and less than 1% increase was due to the surfactant. The increase in the SN ratio of 5 vol% suspensions improved the thermal conductivity, from 11% thermal conductivity increase at SN ratio 0.1:1 to 15% increase at SN

ratio 1:1. Further increase in the surfactant concentration did not change the thermal conductivity value. It is suggested that at 1:1 SN ratio the saturation of the nanoparticle interface with surfactant molecules was achieved and no further improvement to the suspension microstructure occurred at higher surfactant loadings at room temperature.

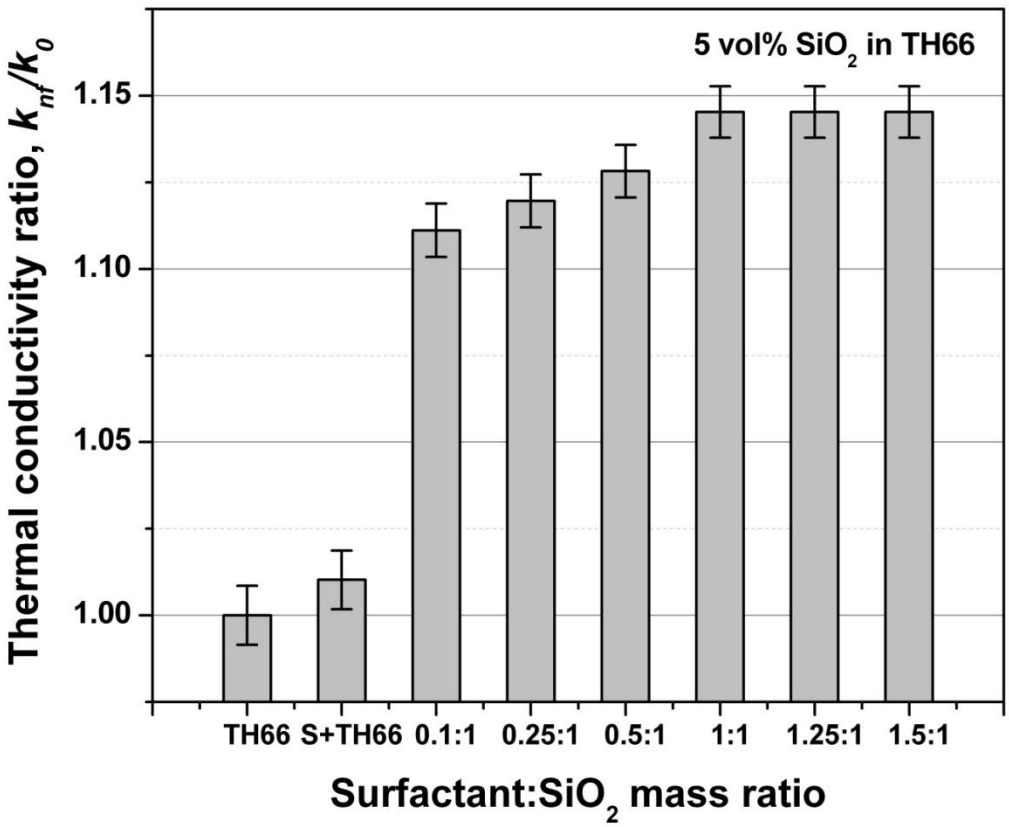

Figure 5. Enhancements in thermal conductivity of 5 vol% SiO_2/TH66 suspensions at various SN ratio. S+TH66 indicates the thermal conductivity measured in base fluid with highest surfactant concentration used in the series (i.e. as in 1.5:1 ratio).

The particle size distributions in diluted suspensions of nanoparticles with SN ratio 0.1:1 and 1:1 were first tested at room temperature (Fig. 6). The suspension with 1:1 SN ratio had an average agglomerate diameter of 350 nm, while the agglomerate sizes in suspension with 0.1:1 ratio were significantly larger (~1250 nm). This data correlates well with viscosity and thermal

conductivity results, confirming that particle agglomeration has an effect on the thermal conductivity, viscosity, and also demonstrates that agglomeration of nanoparticles can be minimized by introducing the adequate amount of proper surfactant.

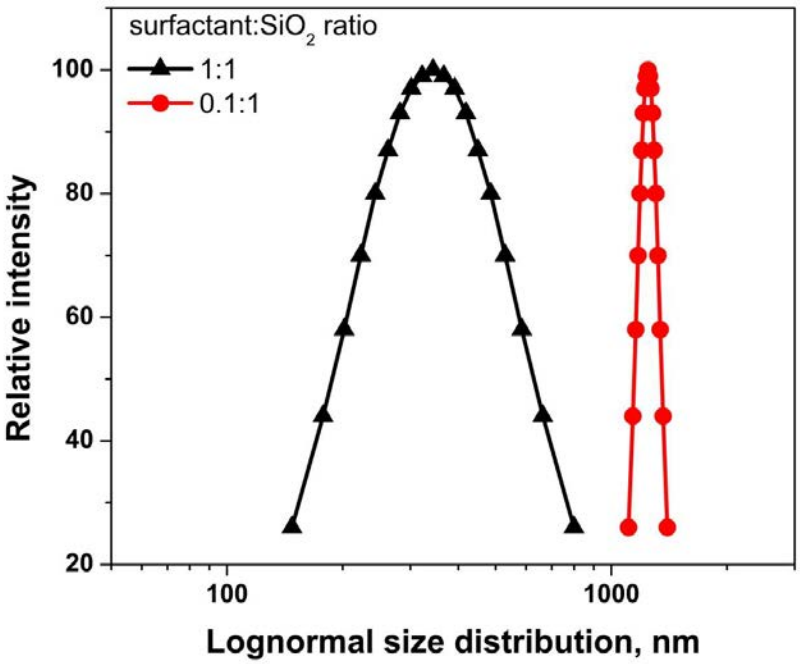

Figure 6. Average agglomerate sizes in suspension with 1:1 (black triangles) and 0.1:1 (red circles) surfactant-to-nanoparticle ratio.

The temperature effect on the average agglomerate size was investigated by measuring the DLS spectra as the suspensions with 1:1 and 0.1:1 SN ratio were heated to 70°C and cooled back to room temperature (Fig. 7). Suspension with 1:1 ratio showed decrease in the agglomerate size with increasing temperature, confirming partial de-agglomeration that was suggested for lower viscosity ratios at elevated temperatures. As the fluid was cooled down to the room temperature the average size of agglomerates changed back to the equilibrium size. Dramatically different behavior is observed in suspensions with 0.1:1 surfactant ratio (Fig. 7). The increase in the temperature resulted in continuous increase of the agglomerate sizes, which confirms the

interpretation of observed continuous viscosity increase at a >65°C as a temperature driven agglomeration of nanoparticles at insufficiently low SN ratios.

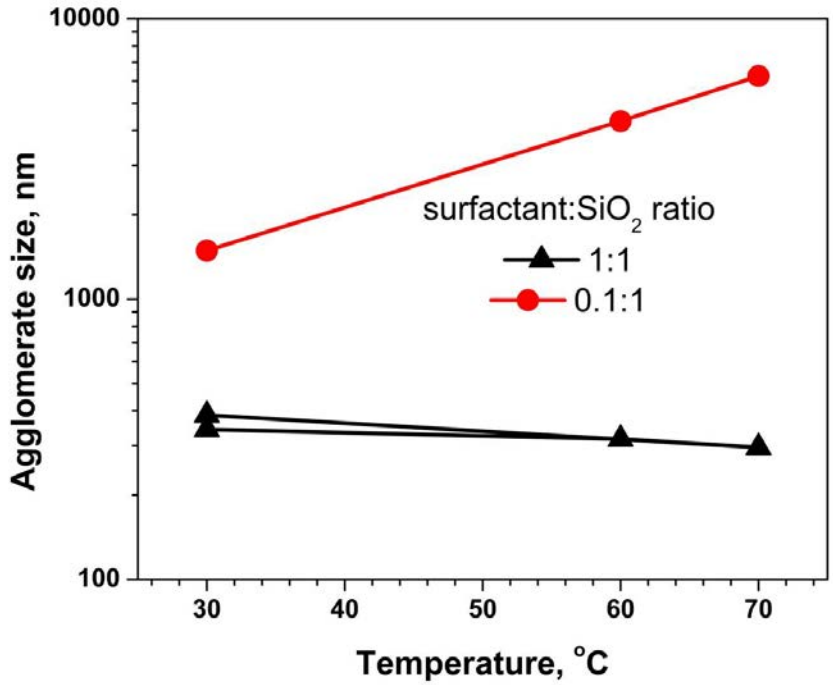

Figure 7. Changes in average agglomerate size with temperatures in suspensions with optimized SN ratio 1:1 (black triangles) and SN ratio 0.1:1 (red circles).

3. Sonication Conditions

The nanofluid preparation procedure can affect the homogeneity and stability of suspension [39]. Amongst various physical dispersing methods the high energy ultrasonic treatment was shown to provide levels of particle de-agglomeration sufficient to get stable nanofluids [40]. The effect of ultrasonic treatment conditions on the viscosity of 5.0 vol% SiO_2 nanofluid were studied for the suspension with SN ratio 1:1. Initial sonication procedures were completed as described for all suspensions (10 x 5 min, < 65°C). The viscosity of nanofluid was not changing from further treatments at this sonication conditions. The treatment cycle was expanded to longer sonications (~10 min) during which the temperature was rising to ~90°C. The viscosity of the

nanofluid, measured soon after sonications, was decreasing as the longer sonication cycles progressed (Fig. 8). The viscosity drop of nearly 50% was achieved after 12 extended sonications. However, after 8 days at rest the viscosity of the suspension retreated to the values that had been established after the initial sonication procedures.

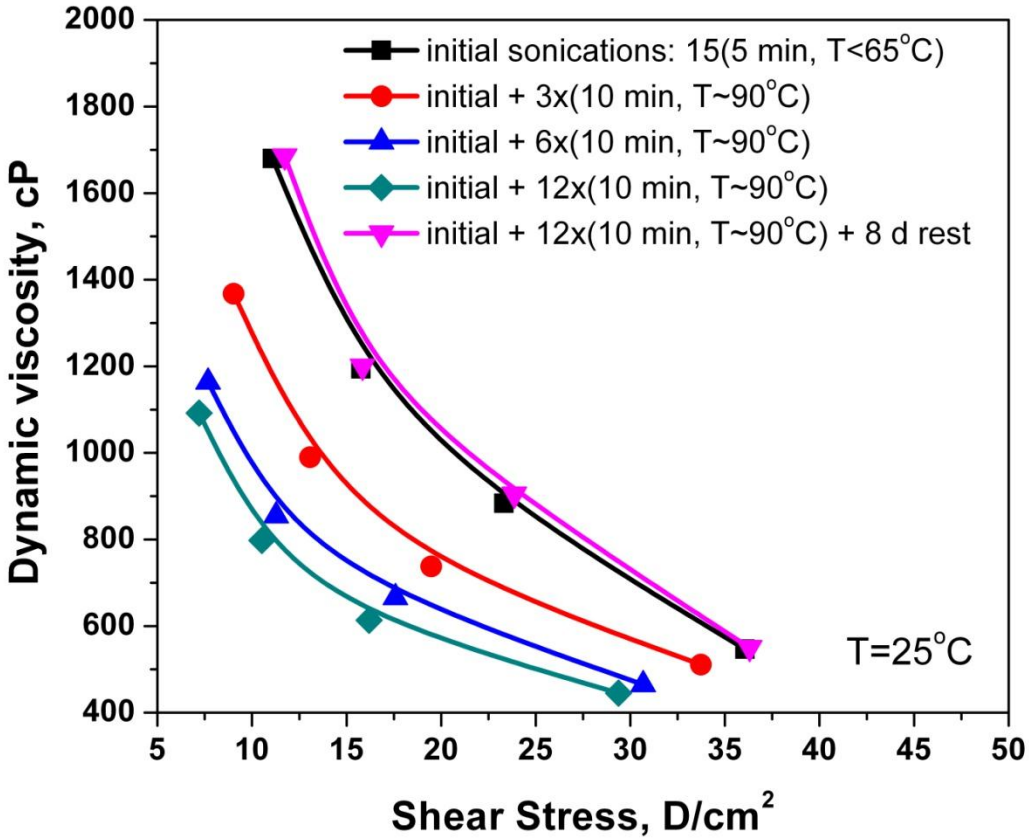

Figure 8. Viscosity at 25°C as a function of shear stress measured after initial and extended ultrasonic treatments.

The high-energy ultrasound waves enhance the kinetic energy of individual nanoparticles that allows overcoming the attraction forces between nanoparticles and break the agglomerates apart. Such a vigorous agitation allowed for non-equilibrium stabilization of smaller nanoparticles/agglomerates that resulted in lower viscosity soon after the extended sonications.

As the system equilibrated the forces affecting dispersion stability balanced out, and the equilibrium agglomerate sizes and characteristic viscosity for the given SN ratio were re-established. The similar equilibration of agglomerate size to the equilibrium value was observed in DLS tests with temperature cycling (Fig. 7).

4. Estimation of the heat transfer efficiency

Since the cooling efficiency of the heat transfer fluids is the main consideration in the current nanofluid development, the ratio of heat transfer coefficients for the suspensions and the base fluid were estimated for fully developed (hydrodynamically and thermally) laminar and turbulent flow regimes using the fluid dynamic equations [26, 41]. The ratio of heat transfer coefficients is a convenient measure for comparison of two fluids flowing in the same geometry and at the same flow rates. In laminar flow regime the heat transfer coefficients are proportional to the thermal conductivity (within the acceptable range of inlet/outlet temperature difference), while in turbulent flow heat transfer coefficients depend on a set of thermo-physical properties [26]. A combination of measured and calculated properties were used in this estimation, as shown in table 1. Introduction of inorganic nanoparticles to the fluids changed the thermo-physical properties: increased the density (ρ), thermal conductivity (k), viscosity (μ), and decreased the specific heat of suspensions (c_p). The percentage increases in thermal conductivity from addition of nanoparticles was reported to be independent on temperature of the fluid [32, 42], so the increase measured at room temperature was used for all temperatures. The viscosity increase was experimentally measured up to 135°C, and for 200°C it was assumed that the Einstein-Bachelor equation applies for viscosity increase. The effective density (ρ_{nf}) and effective specific heat of the nanofluid $(c_p)_{nf}$ at various temperatures were calculated using the rule of mixtures and the

volume concentration of the solid particles (ϕ). The temperature dependence of specific heat and density of the base fluid (TH66) was provided in manufacturer product specifications and the properties for solid silica nanoparticles were assumed constant in the given range of temperatures.

	Thermo-physical properties				Heat transfer coefficient ratio [26, 41]	
Nanoparticle concentration	Thermal conductivity	Dynamic viscosity at 20 D/cm^2	Specific heat	Density	Laminar flow	Turbulent flow
ϕ, vol%	k, W/mK (measured)	μ, cP (measured)	c_p, J/kgK $(c_p)_{nf} = \frac{(1-\phi)(\rho c_p)_0 + \phi(\rho c_p)_p}{(1-\phi)\rho_0 + \phi\rho_p}$	ρ, kg/m^3 $\rho_{nf} = (1-\phi)\rho_0 + \phi\rho_p$	$\frac{h_{nf}}{h_0} \approx \frac{k_{nf}}{k_0}$	$\frac{h_{nf}}{h_0} \approx \left(\frac{\rho_{nf}}{\rho_0}\right)^{4/5} \left(\frac{c_{p\,nf}}{c_{p\,0}}\right)^{2/5} \left(\frac{\mu_{nf}}{\mu_0}\right)^{-2/5} \left(\frac{k_{nf}}{k_0}\right)^{3/5}$
T=25°C						
0	0.117	71.0	1580	1003	1.00	1.00
1.2	0.120	109.0	1553	1023	1.03	0.84
3.6	0.127	149.0	1502	1062	1.08	0.76
5.0	0.131	595.0	1474	1085	1.12	0.41
7.0	0.137	1594.0	1435	1117	1.17	0.27
T=65°C						
0	-	9.7	1720	980	1.00	1.00
1.2	-	12.3	1688	1000	1.03	0.92
3.6	-	15.7	1627	1040	1.08	0.86
5.0	-	35.3	1594	1063	1.12	0.61
7.0	-	158.0	1549	1096	1.17	0.32
T=125°C						
0	-	2.16	1930	937	1.00	1.00
1.2	-	2.41	1890	957	1.03	0.98
3.6	-	2.99	1813	998	1.08	0.93
5.0	-	5.16	1772	1022	1.12	0.75
7.0	-	-	1716	1056	1.17	-
T=200°C						
0	-	0.87	2200	884	1.00	1.00
1.2	-	0.90	2148	905	1.03	1.02
3.6	-	0.95	2050	947	1.08	1.04
5.0	-	0.99	1997	972	1.12	1.06
7.0	-	1.03	1926	1007	1.17	1.09

Table 1. Estimation of heat transfer coefficients in nanofluids from thermo-physical properties.

The ratio of heat transfer coefficients (h_{nf}/h_0) for the nanofluids and the base fluid calculated for different temperatures (Fig. 9) show that the inclusion of nanoparticles in synthetic oil coolant can provide considerable improvement in heat transfer rates at all temperatures when used in laminar flow regime, with the improvements proportional to the particle volume

fractions. Heat transfer coefficients in the turbulent flow regime are strongly dependent on the temperature, and show the benefit of adding nanoparticles only when nanofluid is used at high temperatures. This is mostly due to the significant viscosity increases in nanofluids vs. base fluid. The viscosity of nanofluids vs. base fluids was shown decrease with increasing temperatures and can be further reduced with SN ratio and temporarily with ultrasonic treatment. Therefore heat transfer coefficient improves with temperature for nanofluids and the high temperature applications represent a great outlet for nanofluids cooling potential.

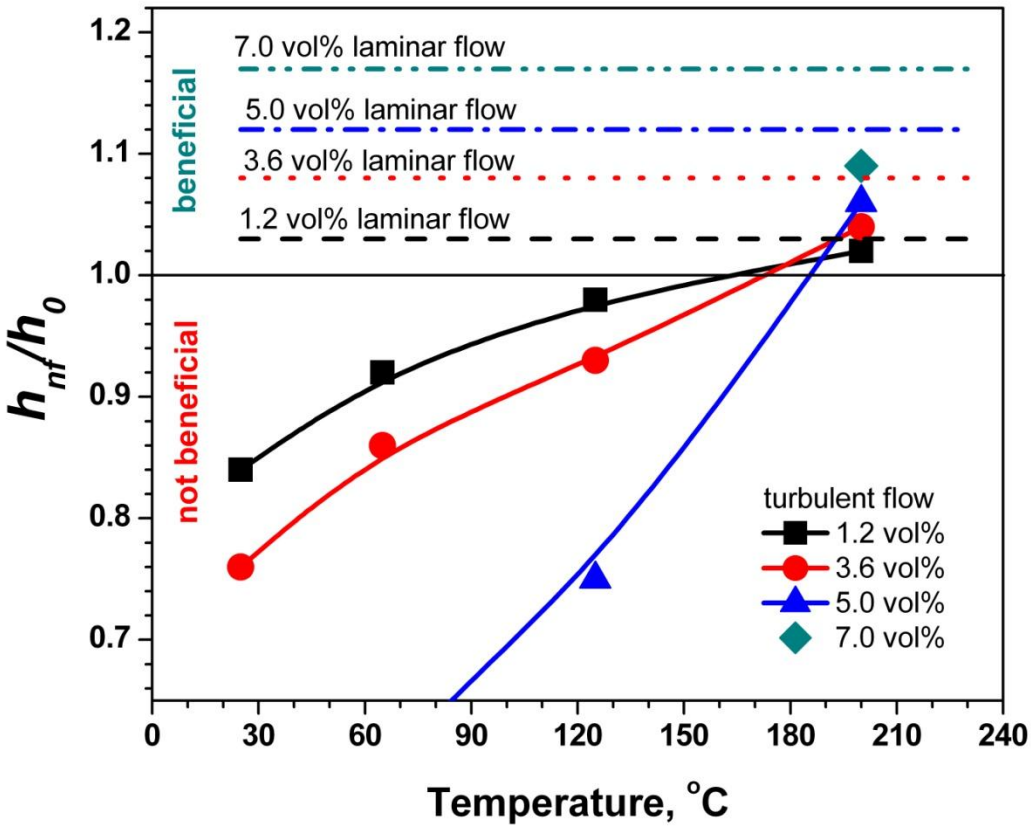

Figure 9. Estimation of the cooling efficiency of SiO_2/TH66 nanofluids as a function of the average temperature at various nanoparticle concentrations for laminar and turbulent flow.

Conclusions

This study demonstrates that addition of inorganic nanoparticles can improve the heat transfer properties of synthetic oil. Stable SiO_2 nanofluids in TH66 prepared with cationic benzalkonium chloride surfactant show linear increase in thermal conductivity with particle concentration in agreement with the effective medium theory. Viscosity of suspensions increases non-linearly with particle concentration and also depends on the surfactant-to-nanoparticle (SN) ratio. The SN ratio defines the average agglomerate sizes as observed with DLS, and affects both viscosity and thermal conductivity of nanofluids. It was demonstrated that at the same particle loadings highly agglomerated suspensions have lower thermal conductivities than well dispersed nanofluids. Optimal SN mass ratio was found to be between 0.5:1 to 1.25:1 for 10 nm SiO_2 particles, which roughly corresponds to monolayer coverage with molecules "laying flat" on nanoparticle surface and compressed monolayer of "standing-up" surfactant. Viscosity ratio (nanofluid vs. base fluid) is temperature dependent, and decreases as the temperature goes up due to reduction in aggregate sizes. The equilibrium agglomerate sizes characteristic to SN ratio can be temporarily reduced by implication of extended sonication times and higher temperatures, which also results in viscosity decrease. If the surfactant concentration is below the "laying flat" monolayer concentration the temperature increase above 65°C induces temperature driven agglomeration and continuous viscosity increase.

The nanofluids are expected to be next generation coolants, and the ability to assess their heat transfer potential from measured thermo-physical properties is extremely important. In this work we demonstrated the sensitivity of the nanofluid thermo-physical properties to concentrations of nanoparticles and surfactant, preparation procedures, and operation temperatures. The heat transfer efficiency of formulated SiO_2 suspensions suggests higher benefits when nanofluids are

used in laminar flow regime or at higher temperatures in turbulent flow regime. Further research of high temperature nanofluids will target thermal stability of surfactant, better control over particle agglomeration, and possibly translation of unique properties of nanomaterials onto the fluid media.

Acknowledgements

This work was supported by US Department of Energy EERE Solar Energy Technology Program – American Recovery and Reinvestment Act (ARRA) funding, Mr. Moravek was partially supported by DOE's Science Undergraduate Laboratory Internship program. Argonne National Laboratory is managed by UChicago Argonne, LLC for US DOE under Contract DE-AC02-06CH11357.

References:

[1] L.Q. Wang, J. Fan, Nanoscale Res. Lett. 5 (2010) 1241.

[2] S. Ozerinc, S. Kakac, A.G. Yazicioglu, Microfluidics and Nanofluidics 8 (2010) 145.

[3] W. Yu, D.M. France, J.L. Routbort, S.U.S. Choi, Heat Transf. Eng. 29 (2008) 432.

[4] D.S. Wen, G.P. Lin, S. Vafaei, K. Zhang, Particuology 7 (2009) 141.

[5] R.A. Taylor, P.E. Phelan, Int. J. Heat Mass Transf. 52 (2009) 5339.

[6] Y.J. Li, J.E. Zhou, S. Tung, E. Schneider, S.Q. Xi, Powder Technology 196 (2009) 89.

[7] X.Q. Wang, A.S. Mujumdar, Int. J. Thermal Sci. 46 (2007) 1.

[8] D.G. Cahill, W.K. Ford, K.E. Goodson, G.D. Mahan, A. Majumdar, H.J. Maris, R. Merlin, S.R. Phillpot, J. Appl. Phys. 93 (2003) 793.

[9] S.K. Das, S.U.S. Choi, H.E. Patel, Heat Transfer Eng. 27 (2006) 3.

[10] S. Kabelac, J.F. Kuhnke, Ann. Assembly Int. Heat Transfer Conf. 13 (2006) KN.

[11] J. Buongiorno, D.C. Venerus, N. Prabhat, T. McKrell, J. Townsend, R. Christianson, Y.V. Tolmachev, P. Keblinski, L.-w. Hu, J.L. Alvarado, I.C. Bang, S.W. Bishnoi, M. Bonetti, F. Botz, A. Cecere, Y. Chang, G. Chen, H. Chen, S.J. Chung, M.K. Chyu, S.K. Das, R.D. Paola, Y. Ding, F. Dubois, G. Dzido, J. Eapen, W. Escher, D. Funfschilling, Q. Galand, J. Gao, P.E. Gharagozloo, K.E. Goodson, J.G. Gutierrez, H. Hong, M. Horton, K.S. Hwang, C.S. Iorio, S.P. Jang, A.B. Jarzebski, Y. Jiang, L. Jin, S. Kabelac, A. Kamath, M.A. Kedzierski, L.G. Kieng, C. Kim, J.-H. Kim, S. Kim, S.H. Lee, K.C. Leong, I. Manna, B. Michel, R. Ni, H.E. Patel, J. Philip, D. Poulikakos, C. Reynaud, R. Savino, P.K. Singh, P. Song, T. Sundararajan, E. Timofeeva, T. Tritcak, A.N. Turanov, S.V. Vaerenbergh, D. Wen, S. Witharana, C. Yang, W.-H. Yeh, X.-Z. Zhao, S.-Q. Zhou, J. Appl. Phys. 106 (2009) 094312.

[12] D.C. Venerus, J. Buongiorno, R. Christianson, J. Townsend, I.C. Bang, G. Chen, S.J. Chung, M. Chyu, H.S. Chen, Y.L. Ding, F. Dubois, G. Dzido, D. Funfschilling, Q. Galand, J.W. Gao, H.P. Hong, M. Horton, L.W. Hu, C.S. Iorio, A.B. Jarzebski, Y.R. Jiang, S. Kabelac, M.A. Kedzierski, C. Kim, J.H. Kim, S. Kim, T. McKrell, R. Ni, J. Philip, N. Prabhat, P.X. Song, S. Van Vaerenbergh, D.S. Wen, S. Witharana, X.Z. Zhao, S.Q. Zhou, Appl. Rheology 20 (2010) 236.

[13] S.Q. Zhou, R. Ni, D. Funfschilling, J. Appl. Phys. 107 (2010) 054317.

[14] A.J. Schmidt, M. Chiesa, D.H. Torchinsky, J.A. Johnson, A. Boustani, G.H. McKinley, K.A. Nelson, G. Chen, Appl. Phys. Lett. 92 (2008) 244107.

[15] S.U.S. Choi, Z.G. Zhang, W. Yu, F.E. Lockwood, E.A. Grulke, Appl. Phys. Lett. 79 (2001) 2252.

[16] S. Shaikh, K. Lafdi, R. Ponnappan, J. Appl. Phys. 101 (2007) 064302.

[17] Y. Hwang, J.K. Lee, C.H. Lee, Y.M. Jung, S.I. Cheong, C.G. Lee, B.C. Ku, S.P. Jang, Thermochim. Acta 455 (2007) 70.

[18] L.F. Chen, H.Q. Xie, Colloid Surf. A-Physicochem. Eng. Asp. 352 (2009) 136.

[19] M.A. Kedzierski, M. Gong, Int. J. Refrigeration-Revue Int. Du Froid 32 (2009) 791.

[20] K. Henderson, Y.G. Park, L.P. Liu, A.M. Jacobi, Int. J. Heat Mass Transfer 53 (2010) 944.

[21] M.A. Kedzierski, ASME Micro Nano Heat Mass Transfer Int. Conf. 2009, Vol 1 (2010) 389.

[22] A.H. Battez, R. Gonzalez, J.L. Viesca, J.E. Fernandez, J.M.D. Fernandez, A. Machado, R. Chou, J. Riba, Wear (2008) 422.

[23] A.H. Battez, J.L. Viesca, R. Gonzalez, D. Blanco, E. Asedegbega, A. Osorio, Wear 268 (2010) 325.

[24] D. Yue-fan, L. Yu-zhen, W. Fo-chi, L. Xiao-xin, L. Cheng-rong, 2010 IEEE Int. Symp. Electric. Insul. (ISEI 2010) (2010) 1.

[25] J.G. Hwang, M. Zahn, F.M. O'Sullivan, L.A.A. Pettersson, O. Hjortstam, L. Rongsheng, J. Appl. Phys. (2010) 014310 (17 pp.).

[26] W. Yu, D.M. France, E.V. Timofeeva, D. Singh, J.L. Routbort, Appl. Phys. Lett. 96 (2010) 213109.

[27] P.K. Namburu, D.P. Kulkarni, A. Dandekar, D.K. Das, Micro Nano Lett. 2 (2007) 67.

[28] R.G. Larson, The Structure and Rheology of Complex Fluids Oxford University Press, Inc., New York, 1999.

[29] R.D. Vold, M.J. Vold, Colloid and interface chemistry. Addison-Wesley Publishing Company, Inc., Reading, Massachusetts, 1983.

[30] E.V. Timofeeva, W. Yu, D.M. France, D. Singh, J.L. Routbort, J. Appl. Phys. (2010).

[31] P.K. Namburu, D.P. Kulkarni, D. Misra, D.K. Das, Exp. Therm. Fluid Sci. 32 (2007) 397.

[32] E.V. Timofeeva, A.N. Gavrilov, J.M. McCloskey, Y.V. Tolmachev, S. Sprunt, L.M. Lopatina, J.V. Selinger, Phys. Rev. E 76 (2007) 061203.

[33] P.E. Gharagozloo, J.K. Eaton, K.E. Goodson, Applied Physics Letters 93 (2008) 103110.

[34] J.C. Maxwell, A Treatise on Electricity and Magnetism. Clarendon, Oxford, UK, 1873.

[35] W. Evans, R. Prasher, J. Fish, P. Meakin, P. Phelan, P. Keblinski, Int. J. Heat Mass Transfer 51 (2008) 1431.

[36] E.V. Timofeeva, J.L. Routbort, D. Singh, J. Appl. Phys. 106 (2009) 014304.

[37] E.V. Timofeeva, W. Yu, D.M. France, D. Singh, J.L. Routbort, J Appl. Phys. 109 (2011) 014914 (5pp).

[38] C.O. Metin, L.W. Lake, C.R. Miranda, Q.P. Nguyen, J. Nanopart. Research 13 (2011) 839.

[39] Y.M. Xuan, Q. Li, Int. J. Heat Fluid Flow 21 (2000) 58.

[40] Y. Hwang, J.K. Lee, Y.M. Jeong, S.I. Cheong, Y.C. Ahn, S.H. Kim, Powder Techn. 186 (2008) 145.

[41] H. Etherington, in: (Ed.)^(Eds.); McGraw-Hill Book Company, Inc., New York, USA, 1958.

[42] D. Singh, E. Timofeeva, W. Yu, J. Routbort, D. France, D. Smith, J.M. Lopez-Cepero, J. Appl. Phys. 105 (2009) 064306.